INTRODUCTION

In materials doped with rare-earth ions, excitation energy does not remain confined to a single ion: it can be transferred non-radiatively from one ion to another. This process is called energy transfer, and it has a decisive influence on the spectral composition, kinetics and efficiency of luminescence [1, 2]. Energy transfer can be either beneficial or detrimental. In beneficial cases, it allows a weakly absorbing ion (the activator) to be excited by means of a strongly absorbing ion (the sensitiser); in detrimental cases, it carries the excitation energy to quenching centres.

The theoretical foundations of energy transfer were laid in the works of T. Förster (1948) and D. Dexter (1953) [3, 4]. Förster showed that for the dipole–dipole interaction the transfer rate is inversely proportional to the sixth power of the donor–acceptor distance. Dexter generalised this theory to multipolar (dipole–quadrupole, quadrupole–quadrupole) and exchange interactions. Later, M. Inokuti and F. Hirayama derived the decay law of donor luminescence for randomly distributed donors and acceptors [5].

Several important types of energy transfer occur in rare-earth ions. In resonant transfer, the donor and acceptor transitions have the same energy; in phonon-assisted transfer, the energy mismatch is compensated by phonons; in cross-relaxation, an excited ion gives part of its energy to a neighbouring ion and both pass into intermediate states; and in migration, the excitation "hops" many times between identical ions [2, 6]. Upconversion processes are also regarded as a distinct type of energy transfer [7].

Energy transfer is of great importance in practical materials. $Yb^{3+}\rightarrow Er^{3+}$ sensitisation serves as the key mechanism for 1.5 μm lasers and amplifiers, $Ce^{3+}\rightarrow Tb^{3+}$ and $Eu^{2+}\rightarrow Mn^{2+}$ transfer for

phosphors, and $Yb^{3+}\rightarrow Er^{3+}/Tm^{3+}$ upconversion for bioimaging [1, 7]. At the same time, in ions such as Nd^{3+}, cross-relaxation leads to concentration quenching and limits the concentration of active ions [8].

Prior estimation of the energy transfer efficiency is the principal tool for optimising material composition. However, this requires a clear understanding of the range of applicability and predictive capabilities of the various models. The aim of this work is to analyse the main theoretical models of energy transfer between rare-earth ions, to calculate the distance and concentration dependence of the transfer efficiency for the dipole–dipole mechanism, and to discuss the results obtained using practical materials as examples.

MATERIALS AND METHODS

Förster–Dexter theory

The rate of dipole–dipole energy transfer between a donor (D) and an acceptor (A) is given by the Förster formula [3]:

$$W_{DA}(R) = (1/\tau_D) \cdot (R_0/R)^6 \quad (1)$$

where τ_D is the donor lifetime in the absence of acceptors, R is the donor–acceptor distance and R_0 is the critical distance, i.e. the distance at which the transfer rate equals the intrinsic decay rate of the donor. The critical distance is determined by the overlap integral of the donor emission spectrum and the acceptor absorption spectrum:

$$R_0^6 = [3\hbar^4 c^4 / (4\pi n^4)] \cdot Q_A \int f_D(E)\, F_A(E)\, E^{-4}\, dE \quad (2)$$

where Q_A is the integrated absorption cross-section of the acceptor transition, and f_D and F_A are the normalised spectral line

shapes [4]. The transfer efficiency for a single donor–acceptor pair is:

$$\eta_{ET}(R) = R_0^6 / (R_0^6 + R^6) \qquad (3)$$

Inokuti–Hirayama model

For acceptors randomly distributed around the donor and in the absence of donor–donor migration, the decay law of donor luminescence is [5]:

$$I(t) = I_0 \exp[-t/\tau_D - \Gamma(1 - 3/s)\,(C_A/C_0)\,(t/\tau_D)^{3/s}] \qquad (4)$$

where s = 6, 8 and 10 correspond to dipole–dipole, dipole–quadrupole and quadrupole–quadrupole interactions, respectively, C_A is the acceptor concentration, $C_0 = 3/(4\pi R_0^3)$ is the critical concentration and Γ is the gamma function. For the dipole–dipole case, $\Gamma(1/2) = \sqrt{\pi}$. The average transfer efficiency is obtained from the integral of the decay curve:

$$\eta_{ET} = 1 - (1/\tau_D) \int_0^\infty I(t)/I_0 \, dt \qquad (5)$$

Calculation parameters

The calculations were performed for a YAG host, in which 1 at. % of dopant corresponds to a concentration of $1.38 \cdot 10^{20}$ cm^{-3}. The mean interionic distance was estimated by the formula $R_m = (3/4\pi N)^{1/3}$. The critical distance was taken as $R_0 = 1.5$ nm; this value falls within the range of 1–2 nm reported in the literature for pairs of rare-earth ions [2, 6]. Expressions (4)–(5) were evaluated by numerical integration.

Experimental verification procedure

To verify the model results experimentally, the decay kinetics of donor luminescence is measured under pulsed excitation. The duration of the excitation pulse must be at least an order of magnitude shorter than the donor lifetime; for rare-earth ions,

nanosecond-pulsed optical parametric oscillators or modulated diode lasers are commonly used. The signal is recorded with a suitable detector and a digital oscilloscope and averaged over 10^3–10^4 pulses. The decay curve of an acceptor-free (donor-only) sample yields τ_D. For a series of samples with different acceptor concentrations, the decay curves are fitted with formula (4) to determine the parameters s and C_0, and hence R_0. For an independent check, R_0 is also calculated from the spectral overlap using formula (2); agreement between the two methods confirms the predominance of the dipole–dipole mechanism [5, 6].

RESULTS

Distance dependence of the transfer efficiency

The results calculated using formulas (1) and (3) are given in Table 1.

Table 1. Dependence of the dipole–dipole energy transfer rate and efficiency on the relative distance R/R_0

R/R_0	R, nm (R_0 = 1.5 nm)	$W_{DA}\tau_D$	η_{ET}, %
0.5	0.75	64.0	98.5
0.8	1.20	3.81	79.2
1.0	1.50	1.00	50.0
1.2	1.80	0.335	25.1
1.5	2.25	0.088	8.1
2.0	3.00	0.016	1.5

The table shows that energy transfer depends very strongly on distance. When the distance is halved relative to R_0, the transfer rate increases 64-fold and the efficiency reaches 98.5%; when the distance is doubled, the efficiency drops to 1.5%. Thus, energy transfer is significant only within the range of approximately $0.5R_0$ – $1.5R_0$; outside this range it is either complete or practically absent.

Effect of concentration

The results calculated using the Inokuti–Hirayama model for various acceptor concentrations are given in Table 2.

Table 2. Effect of acceptor concentration on the energy transfer parameters in a YAG host (R_0 = 1.5 nm, dipole–dipole mechanism)

C_A, at.%	N_A, cm^{-3}	R_m, nm	$\gamma = \sqrt{\pi}\cdot C_A/C_0$	η_{ET}, %
0.5	$6.90\cdot10^{19}$	1.51	1.73	71.7
1	$1.38\cdot10^{20}$	1.20	3.46	88.2
2	$2.76\cdot10^{20}$	0.95	6.92	96.2
5	$6.90\cdot10^{20}$	0.70	17.3	99.3

As the concentration increases from 0.5 at.% to 5 at.%, the mean interionic distance decreases from 1.51 nm to 0.70 nm and the transfer efficiency increases from 71.7% to 99.3%. The calculated donor luminescence decay curves are shown in Fig. 1.

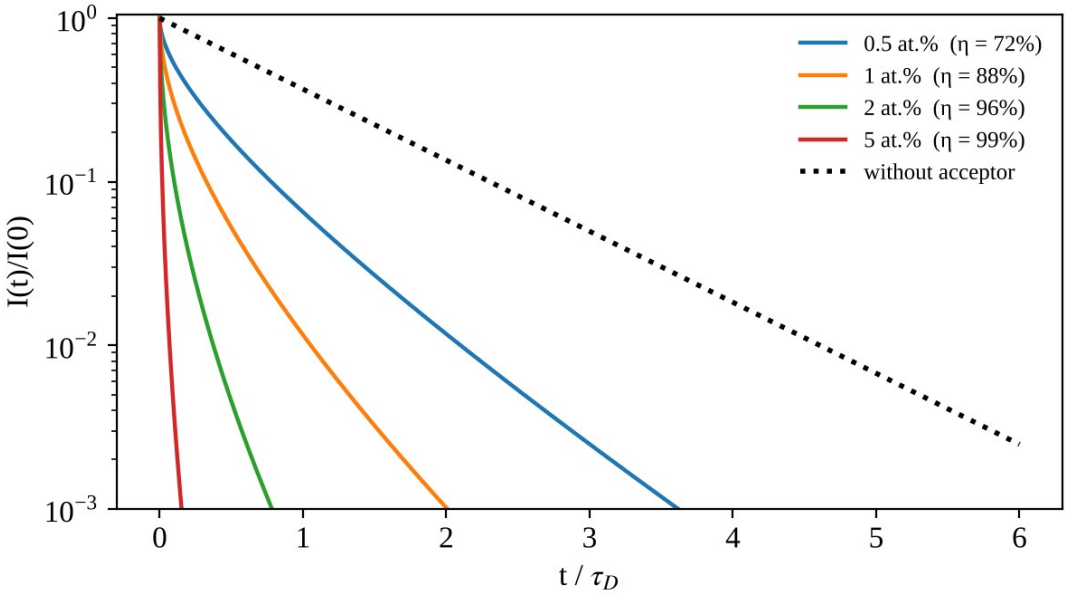


Fig. 1. Donor luminescence decay at various acceptor concentrations according to the Inokuti–Hirayama model (dotted line – without acceptor)

The figure clearly shows the characteristic shape of the decay curves: at early times a steep drop is observed, owing to the fast decay of donors located close to acceptors, followed by a slower, nearly exponential decay due to the contribution of distant donors. Such non-exponential kinetics is the principal experimental

signature of energy transfer. By fitting the initial part of the decay curves on a semi-logarithmic scale with formula (4), the parameter s, i.e. the multipolarity of the interaction, can be determined [5, 6].

The results are also consistent with Table 1: at a concentration of 0.5 at.%, the mean distance is $R_m \approx R_0$, and although the efficiency for individual pairs is around 50%, the average efficiency amounts to 71.7% owing to the acceptors located closer in a random distribution. Hence, in randomly distributed systems, an estimate based on the mean distance considerably underestimates the efficiency.

Concentration dependence of the donor lifetime

It follows from formula (5) that the average (integrated) lifetime of donor luminescence is $\tau_{avg} = (1 - \eta_{ET})\tau_D$. According to the calculations, for acceptor concentrations of 0.5, 1, 2 and 5 at.%, the ratio τ_{avg}/τ_D is 0.283, 0.118, 0.038 and 0.007, respectively. Thus, at a concentration of 5 at.% the donor lifetime is shortened by a factor of almost 140. This result provides the theoretical basis for the simplest experimental method of determining the energy transfer efficiency – comparing the donor lifetimes in samples with and without acceptors. It should be noted that for non-exponential decay the notion of "lifetime" partly loses its meaning; therefore, it is the integrated lifetime that gives the correct result, whereas a time determined from the tail of the curve underestimates the transfer efficiency.

DISCUSSION

Let us consider the results obtained using practical systems as examples. In $Yb^{3+} \rightarrow Er^{3+}$ sensitisation, Yb^{3+} ions have an absorption cross-section at 976 nm roughly an order of magnitude larger than that of Er^{3+}. The $^2F_{5/2}$ level of Yb^{3+} lies in near-resonance with the

$^4I_{11/2}$ level of Er^{3+}, so the transfer is efficient [6, 9]. In practical materials, the Yb^{3+} concentration is chosen to be 5–20 times higher than that of Er^{3+}. According to Table 2, at an acceptor (Er^{3+}) concentration of ~1 at.% the transfer efficiency reaches 85–90%, which agrees with experimental data.

However, back transfer ($Er^{3+}\rightarrow Yb^{3+}$) is also possible in the $Yb^{3+}\rightarrow Er^{3+}$ system. To prevent it, fast multiphonon relaxation from the $^4I_{11/2}$ level to the $^4I_{13/2}$ level of Er^{3+} is required. For this reason, phosphate glasses with high phonon energies are preferred for such systems: in them the lifetime of the $^4I_{11/2}$ level is short, and the energy "has no time to return" [9]. This example clearly illustrates the interplay between energy transfer and multiphonon relaxation.

In real systems, the donor and acceptor transitions are often not in exact resonance. In such cases the energy mismatch ΔE is compensated by the absorption or emission of one or several phonons. According to the theory of Miyakawa and Dexter, the rate of phonon-assisted transfer decreases exponentially with increasing energy mismatch: $W(\Delta E) = W(0)\cdot\exp(-\beta\Delta E)$, where the parameter β depends on the electron–phonon coupling of the host [6]. Consequently, even for pairs at the same distance, the transfer efficiency may differ sharply depending on the phonon spectrum of the host. For example, in $Yb^{3+}\rightarrow Er^{3+}$ transfer the energy mismatch is a few hundred cm^{-1} and is easily bridged by one or two phonons, whereas in $Yb^{3+}\rightarrow Tm^{3+}$ transfer ΔE reaches ~1500 cm^{-1} and the process slows down considerably.

Cross-relaxation, in turn, is in many cases a detrimental process. In the Nd^{3+} ion, the process ($^4F_{3/2}$, $^4I_{9/2}$) → ($^4I_{15/2}$, $^4I_{15/2}$) is close to resonance and converts the excitation energy into phonons. Since the donor and acceptor in this process are ions of the same kind, its rate increases in proportion to the square of the Nd^{3+} concentration.

As a result, in YAG the lifetime of the $^4F_{3/2}$ level decreases appreciably when the Nd^{3+} concentration exceeds 1 at.% [8]. As our calculations show, at a concentration of 2 at.% the interionic distance shrinks to 0.95 nm, and if $R_0 \sim 1$ nm for cross-relaxation, it becomes an efficient quenching channel.

Nevertheless, cross-relaxation can also be beneficial in some cases. In the Tm^{3+} ion, the ($^3H_4$, $^3H_6$) → ($^3F_4$, $^3F_4$) cross-relaxation produces two excited ions in the $^3F_4$ level from a single photon absorbed at 790 nm. This "two-for-one" process brings the quantum efficiency of 2 μm Tm^{3+} lasers close to 200%, and its realisation requires a high Tm^{3+} concentration (3–6 at.%) [1, 10]. The same principle is also used in down-conversion phosphors.

When analysing the mechanism of concentration quenching, migration between donors must also be taken into account. If transfer between identical ions is fast, the excitation "wanders" through the lattice and reaches quenching centres such as crystal defects or uncontrolled impurities (e.g. OH^- groups, Fe^{2+}, Cu^{2+}) [2, 11]. In this case, quenching depends not only on the active-ion concentration but also on the purity of the material. For this reason, particular attention is paid to the purity of raw materials and to the removal of OH^- groups in the synthesis of highly efficient luminescent materials.

One of the modern approaches to increasing energy transfer efficiency is the use of nanostructured materials. In core–shell nanoparticles, the sensitiser and activator ions are placed in different layers, which makes it possible to control the transfer distance and to reduce surface quenching [7]. To describe the energy transfer mechanism correctly in such materials, the Inokuti–Hirayama model must be generalised to restricted geometries.

The limitations of the model used in this work should also be noted. Formula (4) assumes the absence of migration between donors and a random distribution of acceptors. If the dopants form clusters or if fast migration occurs between donors, the decay kinetics is described by the Yokota–Tanimoto or Burshtein models [6]. Furthermore, in real crystals ions can occupy only lattice sites; therefore, at very short distances the continuous-distribution approximation breaks down and discrete summation must be used.

CONCLUSIONS

1. The main mechanisms of energy transfer between rare-earth ions (resonant and phonon-assisted transfer, cross-relaxation, migration, upconversion) and the Förster–Dexter and Inokuti–Hirayama models describing them have been analysed.

2. It has been shown that the dipole–dipole transfer efficiency depends very strongly on distance: 98.5% at $R = 0.5R_0$, 50% at $R = R_0$ and 1.5% at $R = 2R_0$; transfer is practically significant only within the range $0.5R_0 – 1.5R_0$.

3. It has been calculated that in a YAG host with $R_0 = 1.5$ nm, as the acceptor concentration increases from 0.5 at.% to 5 at.%, the average transfer efficiency increases from 71.7% to 99.3%, and donor luminescence exhibits non-exponential kinetics.

4. The results have been discussed using the examples of $Yb^{3+}\rightarrow Er^{3+}$ sensitisation, concentration quenching in Nd^{3+} and beneficial cross-relaxation in Tm^{3+}. The results can be applied to optimising dopant concentrations in luminescent and laser materials.

REFERENCES

1. Blasse G., Grabmaier B.C. Luminescent Materials. – Berlin: Springer, 1994. – 232 p.

2. Henderson B., Imbusch G.F. Optical Spectroscopy of Inorganic Solids. – Oxford: Clarendon Press, 1989. – 645 p.
3. Förster T. Zwischenmolekulare Energiewanderung und Fluoreszenz // Annalen der Physik. – 1948. – Bd. 437. – S. 55–75.
4. Dexter D.L. A theory of sensitized luminescence in solids // Journal of Chemical Physics. – 1953. – Vol. 21. – P. 836–850.
5. Inokuti M., Hirayama F. Influence of energy transfer by the exchange mechanism on donor luminescence // Journal of Chemical Physics. – 1965. – Vol. 43. – P. 1978–1989.
6. Liu G., Jacquier B. (eds.) Spectroscopic Properties of Rare Earths in Optical Materials. – Berlin: Springer, 2005. – 550 p.
7. Auzel F. Upconversion and anti-Stokes processes with f and d ions in solids // Chemical Reviews. – 2004. – Vol. 104. – P. 139–173.
8. Lupei V., Lupei A. Nd:YAG at its 50th anniversary: still to learn // Journal of Luminescence. – 2016. – Vol. 169. – P. 426–439.
9. Desurvire E. Erbium-Doped Fiber Amplifiers: Principles and Applications. – New York: Wiley, 1994. – 770 p.
10. Kenyon A.J. Recent developments in rare-earth doped materials for optoelectronics // Progress in Quantum Electronics. – 2002. – Vol. 26. – P. 225–284.
11. Bünzli J.-C.G., Eliseeva S.V. Lanthanide NIR luminescence for telecommunications, bioanalyses and solar energy conversion // Journal of Rare Earths. – 2010. – Vol. 28. – P. 824–842.